Effect of fuel properties on primary breakup and spray formation studied at a gasoline 3-hole nozzle

L. Zigan*, I. Schmitz, M. Wensing and A. Leipertz
Lehrstuhl für Technische Thermodynamik, Universität Erlangen-Nürnberg
Erlangen Graduate School in Advanced Optical Technologies (SAOT)
Am Weichselgarten 8, D-91058 Erlangen, Germany

Abstract

The initial conditions of spray atomization and mixture formation are significantly determined by the turbulent nozzle flow. In this study the effect of fuel properties on primary breakup and macroscopic spray formation was investigated with laser based measurement techniques at a 3-hole research injector in an injection chamber. Two single-component fuels (n-hexane, n-decane), which are representative for high- and low-volatile fractions of gasoline with sufficient large differences in viscosity, surface tension and volatility were studied. Integral and planar Mie-scattering techniques were applied to visualize the macroscopic spray structures. To characterize the microscopic spray structure close to the nozzle exit a high resolving long distance microscope was used. For deeper insight into primary breakup processes with effects on global spray propagation the range of Reynolds (8,500-39,600) and liquid Weber numbers (15,300-44,500) was expanded by variation of the fuel temperature (25 °C, 70 °C) and injection pressure (50 bar, 100 bar). The spray is characterized by strong shot-to-shot fluctuations and flipping jets due to the highly turbulent cavitating nozzle flow. Significant differences in microscopic spray behavior were detected at valve opening and closing conditions, whereas during the quasi-stationary main injection phase the spray parameters cone angle and radial spray width show a plateau-trend for the different fuels. The radial spray width at the nozzle exit as well as the microscopic cone angle decrease by trend with higher Reynolds and Weber numbers at early injection phases leading to increased macroscopic spray propagation. The fine scale analysis showed chaotic structure of the disintegrating jet at the beginning injection phase with intense ligament formation depending on fuel properties and the turbulent cavitating nozzle flow.

Introduction

Spray guided Direct Injection Spark Ignition (SG-DISI) engines require fast fuel atomization and evaporation with a reproducible placement of fuel vapour close to the spark plug to ensure a stable ignition of the air/fuel mixture. With the application of modern regenerative and synthetic fuels the mixture formation appeared different compared to gasoline, mainly due to changed evaporation behavior of high and low boiling fuel fractions. This fuel dependent evaporation and mixing behavior of different volatility classes is studied in transparent engines, see, e.g. [1]. Also secondary spray breakup and droplet momentum distribution is controlled by fuel evaporation behavior [2]. The initial conditions of spray atomization and mixture formation are significantly determined by the design of the nozzle and the resulting turbulent two-phase nozzle flow, which is also dependent on fuel properties. Especially for diesel-injection at elevated pressures the influence of cavitation on the macroscopic spray breakup was studied in detail [3,4,5,6]. In [5] two realistic metal nozzle geometries (cylindrical, conical) were investigated under Diesel-like conditions for different injection pressures resulting in a wide range of turbulent flow regimes (i.e. Reynolds numbers) as well as cavitating and non-cavitating flow with changed macroscopic spray behavior. The conical nozzle shows less distinct geometric cavitation with decreasing macroscopic cone angle when the atomization regime is shifted from turbulent to cavitating flow. For the cylindrical nozzle cavitation is more pronounced when increasing the injection pressure which is leading to a larger spray cone angle.

In [6,7] transparent two-dimensional model nozzles and large scale nozzles were used with water to analyze the onset of cavitation. In [7] the influence of Reynolds and cavitation numbers on cavitation in the nozzle and resulting liquid jet was investigated by varying the nozzle size, fluid properties and liquid flow rate. The cavitation and the liquid jet at the nozzle exit are not strongly affected by Reynolds number but by the cavitation number. The collapse of cavitation bubbles at the nozzle exit induces strong turbulence which supports ligament formation. For geometric cavitation conditions the spray cone angle increases with smaller surface tension (of light oil compared to water). An increase of the fluid temperature also leads to a large spray angle for water. Reference [6] is focused on string cavitation (vortex type cavitation) which in contrast to geometrical cavitation strongly supports spray instabilities like cycle-to-cycle variations. Those vapour structures are usually found in the bulk of the liquid fuel in the region where vortical flow structures exist. The formation of the vapour volume

* Corresponding author: lars.zigan@cbi.uni-erlangen.de

fraction at a certain location is very irregular and their interaction with the mean flow is poorly understood. Its presence in the injection hole leads to an increase of the spray cone angle at the side of its occurrence related to the hole axis.

In [8] the characteristics of Diesel fuel and Biodiesel for turbulent flow, cavitating flow and hydraulic flip were investigated for large scale transparent nozzles. For the stationary flow the occurrence of geometrical cavitation and hydraulic flip is at constant Weber numbers for both Diesel and Biodiesel but for Biodiesel it starts already at much lower Reynolds numbers. No effect of fuel properties on resulting spray geometry was reported and the cavitation patterns at the orifice wall inside the nozzle are very similar. The resulting droplet sizes for cavitation conditions are smaller compared to the turbulent, non-cavitating flow.

However, for real-size DISI multi-hole nozzles there is a lack of data concerning influence of geometry and fuel properties under varied injection conditions on nozzle outflow and macroscopic spray behavior. Fundamental studies of fuel-dependent nozzle flow and spray behavior are required for the optimization of spray guided direct injection concepts especially in combination with modern synthetic and regenerative fuels. The application of simplified model fuels gives deeper insight in spray-sub processes with a high relevance for modeling approaches. However, the prediction of the spray behavior for different fuel properties is hardly considered in modeling approaches since turbulence and cavitation conditions are less covered [9,10]. In this study a 3-hole research injector was examined in an injection chamber with Mie-imaging techniques to study fuel impact as well as the influence of injection pressure and fuel temperature on primary breakup and macroscopic spray behavior.

Materials and Methods

Injection chamber and tested fuels

The spray experiments were conducted in an optical accessible injection chamber. The chamber pressure was set to 1 bar to decrease the influence of back-pressure on primary atomization. A constant air flow through the injection chamber heats the chamber and scavenges it from one injection to another (flow velocity <0.1 m/s). The fuel and the injector were conditioned to 70°C and the injection pressure was set to 50 bar and 100 bar with a flexible fuel system. The injection repetition rate was set to 1 Hz. The investigated injector is based on a 6-hole solenoid injector of engine series application (Continental XL2), however, the nozzle was changed to a 3-hole plate for better optical access of the single fuel jets. The injector shows a characteristic turbulent flow behaviour also for low injection pressures (for more details see [11]) and string cavitation which is advantageous for a rapid atomization. The injection duration was kept constant for all investigated fuels at 1,000 µs resulting in an injected mass of approximately 9 mg/pulse (100 bar) and 6.6 mg/pulse (50 bar). The bore diameter of the nozzle holes is approximately 250 µm.

Two single component fuels (n-hexane, n-decane) with comparably large differences in viscosity, surface tension and volatility were studied, see table 1. The range of the fuel properties is representative for a multi-component gasoline fuel. Furthermore, fuel temperature (25 °C, 70 °C) was varied to affect atomization by systematically changing the Reynolds and Weber numbers for an increased insight into spray sub-processes. In table 1 the fluid properties are given for 65 °C since for hexane the boiling point is at 68 °C and therefore no liquid properties are defined at 70 °C.

The calculated Ohnesorge (Oh), liquid Weber (We_L) and Reynolds (Re_L) numbers which describe the primary spray breakup characteristics are defined according [12]:

$$Oh = \frac{\eta_L}{\left(\rho_L \sigma d_0\right)^{0.5}} \tag{1}$$

$$We_L = \frac{\rho_L d_0 u_L^2}{\sigma} \tag{2}$$

$$Re_L = \frac{d_0 u_L}{\nu_L} \tag{3}$$

The included properties are liquid density ρ_L, kinematic viscosity ν_L and surface tension σ as well as velocity u_L and nozzle bore diameter d_0. Injection velocities were calculated from the measured averaged spray penetrations (at 100 µs, see Figure 3) to be approximately 60-64 m/s (at 100 bar) which is decreasing with higher viscosity depending on the applied fuel and injector temperature. The velocity inside the nozzle would be much higher but can hardly be estimated due to reduction of the outflow cross section by cavitation. The resulting non-dimensional numbers are given in table 2.

A small Reynolds number for n-decane indicates a lower turbulent intensity affecting the fuel droplet breakup. This is also reflected by a small Weber number which is determined by a large surface tension and the fuel density leading to a slow breakup process. The cavitation number is not considered since the critical cavitation number is not known for the nozzle at the tested boundary conditions.

Spray visualization technique

The spray process was examined with flash lamps as well as laser based macroscopic and microscopic imaging techniques. To characterize the global spray propagation, integral Mie-Imaging with flash lamps was applied, see Figure 1a. The scattered light was detected perpendicular to the measurement plane with a CCD-camera with 1,280×1,024 pixels and a dynamic range of 12 bit.

Additionally, to describe the liquid fuel distribution of one liquid jet in axial direction a light sheet Mie scattering technique was used. The beam of a pulsed Nd:YAG-Laser (532 nm) was formed into a light sheet (thickness approximately 500 µm) by an arrangement of cylinder lenses. Averaged images were calculated from 32 single-shot images. The average spray penetration was calculated for each measured point in time. With the application of a long-distance microscope (Questar Corporation, QM-100) the microscopic jet disintegration close to the nozzle exit (see Figure 1b) was studied in detail in a region of 1.8 x 1.4 mm ca. 1 mm below the exit with a spatial resolution of 1.4 µm/pixel. The injection chamber was positioned on a traverse system to adjust the measurement region. Average images and liquid fuel probability density distributions were calculated from 32 single shot images for each time step. Furthermore, the spray cone angle and radial spray width at the outlet of the nozzle were evaluated for microscopic images. An In-house software was used to calculate the spray angle from two regression lines based on 50 equidistant lines intersecting with the spray edges. For the evaluation of the single images the spray edges were smoothened by a 3×3 median filter.

Results and Discussion

Macroscopic Spray Analysis

In general, the investigated 3-hole injector is characterized by a rapid atomization which is preferable for a fast mixture formation. However, an unsteady spray behavior and single spray fluctuations were observed leading to strong jet-to-jet interactions. Therefore, the spray is not showing a hollow cone structure. Figure 2 gives exemplary single shot images which are presented for atmospheric chamber pressure. For low back-pressure the primary breakup is is less affected by aerodynamic processes the nozzle flow is dominating the disintegration of the single jets into a fine thin spray.

In Figure 3 one single jet is illuminated to study the macroscopic structure of the spray with its large-scale liquid surface perturbations. Due to the strong shot-to-shot fluctuations of the single jets a statistical analysis was conducted. The fuel dependent structure of the jet at the left side is presented by averaged images. It is noted that laser light is also partially scattered by the other two jets which are propagating into the illumination plane leading to a weak signal at the right side. Especially the opening phase of the injector is dominated by chaotic spray behavior generated by the lifting needle and the resulting turbulent flow inside the micro sac hole [11]. This is more pronounced for n-decane leading to a broader spray and intensified fuel-air interaction with a reduced macroscopic penetration, whereas the spray of the heated n-hexane is characterized by a reduced radial expansion of the single jets and increased penetration. Dominating is the fuel viscosity determining the injection velocity which is correlating with spray shape and penetration, see Figure 4.

The resulting larger Reynolds number for the heated n-hexane compared to cold n-decane (increased by a factor of 3) and larger Weber number (increased by a factor of 1.5) leads to an increased macroscopic spray length of approximately 12 % also at very early injection phases, e.g. for 200 µs after visible start of injection (a. v. SOI). Obviously, the spray evaporation has a minor role in liquid fuel propagation under these conditions as the momentum of the high volatility fuel n-hexane seems to be maintained. The effect of primary breakup on the spray shape is described for the microscopic spray close to the nozzle in the next section.

Microscopic Spray Analysis

In Figure 5 the jet disintegration close to the nozzle is presented by characteristic single shot images. Distinct differences in microscopic spray behavior were detected at valve opening and closing conditions. Then, due to the needle movement the turbulence in the cavitating flow in the micro sac hole is increased and a chaotic spray behavior with large scale structures in the liquid phase results. During the ‘quasi-stationary’ main injection phase between 400 µs and 1,000 µs (when the needle is fully lifted) the flow is getting more ‚stable‘, i.e. the disintegrating jet shows a more homogeneous structure with fine-scale surface perturbations, but the shot-to-shot fluctuations are still apparent. The selected time interval is finer at the start of injection to analyze the early spray which is drastically influencing the macroscopic spray behavior at later time points.

For n-decane the spray shows a block-like structure until 20 µs and the disintegration is delayed compared to n-hexane. The velocity vector at the nozzle outlet is depending on the fluid dynamics close to the nozzle wall and on cavitation and turbulence. For n-decane the spray structure is more chaotic at early observation times with a higher probability of large scale ligaments and clusters compared to the n-hexane spray which is characterized by very fine-scale structures. This can be a consequence of the reduced turbulence intensity (Reynolds numbers) for n-decane due to high fuel viscosity and slightly reduced injection velocity, see also [10]. Additionally, a higher surface tension is enhancing spray stability against breakup and therefore delaying the atomization. An increased fuel temperature supports spray breakup since viscosity and surface tension is significantly reduced and so finer ligament structures are resulting. Additionally, large hollow structures appear frequently inside the liquid bulk flow of the single jets, which can be a sign of string cavitation leading to vapour patterns which are swapping within the nozzle bore from one side to the other (see Figure 5, n-decane at 800 µs). Especially, for n-decane this behaviour is distinct. This can also be an explanation for the strong cycle-to-cycle fluctuations of the single jets and spray flipping (i.e. bending of the jet due to cavitation) [6].

Also the radial spray width at the nozzle outlet increases by trend with reduced Reynolds and liquid Weber numbers, see Figure 6. The values were determined in a small region of 40 pixels length downstream in the near-nozzle region as indicated in the diagram. The average radial spray width is increasing at early injection phases and reaches its maximum between 40 µs (n-hexane) and 50 µs (n-decane). Up to 300 µs the trend shows a plateau and then decreasing again. The average radial spray width at the nozzle outlet is approximately 25 % larger for n-decane compared to n-hexane at a fuel temperature of 25 °C. After 400 µs the trend is converging for both fuels. For the heated fuels the average radial spray width is slightly reduced. Between 500 µs and 1,000 µs the average values show a quasi-stationary behavior in accordance to the structural behavior described in Figure 5. Exemplarily, for n-hexane at 25 °C fuel temperature the rms-values (root mean square) are given which are representative for the strong fluctuations of the spray shape. Between 500 µs and 1,000 µs the rms-values of the radial spray width are approximately 0.21 mm and are decreasing to 0.11 mm for a fuel temperature of 75°C. The n-decane sprays show a very similar behavior. After 1,100 µs the radial spray width decreases again due to throttle effects while the needle closes.

The microscopic spray angle is determining the macroscopic spray propagation significantly. The angles were determined for the probability density functions (pdf) of the liquid fuel distribution. Additionally, rms values are calculated from 32 single shot images to describe the flipping jet. At early injection times the spray angle is very large and decreases until 400 µs a. v. SOI when the trend shows a plateau between 400 µs and 1,000 µs. Basically, this is in accordance to the results reported in [5] where macroscopic cone angles were measured at 60 % of the maximum penetration length for a Diesel injection. In our measurements also a strong dependency on fuel properties and internal nozzle flow was detected similar to the trend of the radial spray width. A clear trend depending on fuel properties is visible also at later times of injection (500-1,000 µs) with an increasing microscopic spray angle for increasing kinematic viscosity and surface tension. The maximum spray angles were calculated for n-decane at 25°C fuel temperature to be 5-7° higher compared to n-hexane for a fuel temperature of 75 °C. The rms-values are also decreasing with increased temperature, e.g. for n-hexane from 5.7° (25 °C) to 5.1° (70 °C) at 500 µs. Those results are in accordance to the macroscopic single jet angles and penetrations shown in Figures 3 and 4. A larger microscopic spray angle therefore leads to a broader macroscopic jet with shorter spray length.

In general, these results show a contrary trend to the experiments described in [7] since in our experiments the spray cone angle is decreasing with smaller surface tension by changing the fuel and additionally, a decreased spray angle for higher fluid temperature occurs. However, different nozzle geometries (e.g. L/D ratios) as well as the atomization regime (the pressure in [7] is 300 bar) can be the reason for the different behavior. Also the presence of string cavitation due to the turbulent vortex flow can contribute to this behavior.

For an injection pressure of 50 bar the microscopic spray width and near-nozzle spray cone angle is significantly reduced compared to 100 bar injection pressure. In Figure 8 the spray angle depending on fuel and flow properties is given as a function of Reynolds and Weber numbers. Averaged microscopic spray angles were calculated for the quasi-stationary injection phase (500-1,000 µs). The multiplication of the non-dimensional liquid Weber and Reynolds numbers shows a linear behavior of the averaged spray angles for both tested injection pressures with a steeper slope for 50 bar.

The microscopic spray cone angle is more than 30% higher when the pressure is increased from 50 to 100 bar. This is in accordance to [5] where the macroscopic spray angle is increasing with higher injection pressure (i.e. larger Reynolds and therefore also larger cavitation numbers) for a cavitating nozzle. The double injection pressure (300 to 600 bar) leads to an approximately 15% larger cone angle when cavitation begins and for a less cavitating conical nozzle, the cone angle decreases with an increase in pressure. Therefore, it can be concluded that for the investigated nozzle the microscopic spray angle is larger for increased Reynolds and Weber numbers if the pressure is increased due to the higher cavitation tendency. However, the spray angle is reduced for both tested pressures with larger Reynolds and Weber numbers if the fluid properties viscosity and surface tension are reduced which can be ascribed to effects of the fluid properties on the flow behavior.

Summary and Outlook

In the present paper the effect of fuel properties on the primary breakup and macroscopic spray formation was examined with integral and planar Mie-scattering techniques at a 3-hole nozzle in an injection chamber. The injector is characterized by a rapid atomization without a hollow cone structure but intense jet-to-jet interactions. This is caused by the turbulent cavitating nozzle flow leading to spray flipping and large-scale liquid surface perturbations. Two single-component fuels (n-hexane, n-decane) with sufficient large differences in viscosity, surface tension and volatility were studied. For deeper insight into primary breakup processes the range of Reynolds (8,500-39,600) and liquid Weber numbers (15,300-44,500) was expanded by variation of the fuel temperature (25 °C, 70 °C) and injection pressure (50 bar, 100 bar). In general, the macroscopic spray was characterized by a larger spray width and shorter penetration for n-decane in comparison to n-hexane. The spray length further increased when the fuel was heated to 70°C. This global spray behavior is strongly determined by the primary breakup. Especially at valve opening conditions for n-decane a chaotic structure of the disintegrating jet with large scale surface perturbations, ligaments and clusters was resulting. The n-hexane spray showed a faster breakup with fine scale structures due to higher turbulence intensity and a reduced radial spray width and microscopic spray cone angle at the nozzle exit. An increased fuel temperature further promoted breakup and reduces radial spray width and spray cone angle of the single jets. During the 'quasi-stationary' main injection phase between 400 µs and 1,000 µs when the needle is fully lifted the flow was getting more ‚stable', i.e. the disintegrating jet showed a more homogeneous structure with fine-scale liquid surface perturbations. During this injection phase a clear trend depending on fuel properties was visible with increasing microscopic spray angle for increasing kinematic viscosity and surface tension. For an injection pressure of 50 bar the microscopic spray width and near-nozzle spray cone angle was 30% smaller compared to a 100 bar injection pressure due to reduced cavitation tendency. For both injection pressures the microscopic spray angle showed a linear function if scaled to the product of Reynolds and Weber numbers for the tested injection conditions. The data serves for inclusion of fuel property effects on turbulence and cavitation in atomization models. A comparison with LES calculations and transparent nozzle experiments can give deeper insight into the atomization process. Further fine scale structure analysis is necessary to correlate turbulence quantities with resulting droplet sizes and velocities.

Acknowledgement

The authors gratefully acknowledge the financial support for parts of this work from the Erlangen Graduate School in Advanced Optical Technologies within the framework of the German Excellence Initiative by the German Research Foundation (DFG). The authors would also like to thank Dr. Jerome Helie (Continental Automotive SAS) and Dr. Jun-Mei Shi (Continental Automotive GmbH) for technical support and the stimulating discussions.

References

[1] Krämer, H., Einecke, S., Schulz, C., Sick, V., Nattrass, S. R. and Kitching, J. S., *Simultaneous Mapping of the distribution of different fuel volatility classes using tracer-LIF tomography in an IC engine*. *SAE paper No. 982467*, 1998.

[2] Zigan, L., Schmitz, I., Flügel, A., Wensing, M. and Leipertz, A., *Influence of fuel properties on spray formation and evaporation measured on a piezoelectric injector for second-generation gasoline direct injection Proc. Injection systems for IC engines, IMECHE,* London, 2009.

[3] Fath, A., Münch, K.-U. and Leipertz, A., *Spray Break-Up of Diesel Fuel Close to the Nozzle*. *ILASS'1996*, 1996.

[4] Badock, C., Wirth, R., Fath, A. and Leipertz, A., *Investigation of cavitation in real size diesel injection nozzles*. *International Journal of Heat and Fluid Flow 20*, pp.538-544 (1999).

[5] Payri, F., Bermúdez, V., Payri, R. and Salvador, F. J., *The influence of cavitation on the internal flow and the spray characteristics in diesel injection nozzles*. *Fuel 83*, 419-431 (2004).

[6] Andriotis, A., Spathopoulou, M. and Gavaises, M., *Effect of Nozzle Flow and Cavitation Structures on Spray Development in Low-speed Two-Stroke Diesel Engines*. *CIMAC Congress 2007,* Vienna, 2007.

[7] Sou, A., Hosokawa, S. and Tomiyana, A., *Effects of cavitation in a nozzle on liquid jet atomization*. *International Journal of Heat and Mass Transfer 50*, 3575-3582 (2007).

[8] Park, S. H., Suh, H. K. and Lee, C. S., *Effect of Cavitating Flow on the Flow and Fuel Atomization Characteristics of Biodiesel and Diesel Fuels*. *Energy Fuels 22*, 605-613 (2008).

[9] Stiesch, G. *Modeling Engine Spray and Combustion Processes*, Berlin; Heidelberg; New York; Barcelona; Hongkong; London; Mailand; Paris; Singapur; Tokio: Springer 2004.

[10] Shi, J.-M. and Arafin, M. S., *CFD investigation of fuel property effect on cavitating flow in generic nozzle geometries*. *ILASS-Europe 2010, 23rd Annual Conference on Liquid Atomization and Spray Systems,* Brno, 2010.

[11]Shi, J.-M., Wenzlawski, C., Helie, J., Nuglisch, H. and Cousin, J., *URANS & SAS analysis of flow dynamics in a GDI nozzle. ILASS-Europe 2010, 23rd Annual Conference on Liquid Atomization and Spray Systems*, 2010.

[12]Lefebvre, A. H. *Atomization and Sprays*, Hemisphere Publishing Corporation, 1989.

Table 1. Liquid fuel properties (1 bar) [a, b, c]

	n-hexane (25°C)	n-hexane (65°C)	n-decane (25°C)	n-decane (65°C)	gasoline (25°C)
density (kg/m³)	656	618	717	689	720-740
kinem. viscos-ity (x 10^{-6} m²/s)	0.446	0.339	1.223	0.765	0.530
vapour pressure (bar)	0.199	0.889	0.002	0.019	0.045-0.064
surface tension (N/m)	0.018	0.013	0.023	0.019	0.022

[a] calculated: fluidat V1.22/5.70, available at <http://www.fluidat.com>.
[b] J.A. Dean, Lange's Handbook of Chemistry, McGraw-Hill, Inc., 1999, p.5.91-5.104.
[c] V. Wagner, J. Goldlücke, O. Seelig, A. Leipertz, Engine Combustion Processes (VI. Congress), ESYTEC, 2003, p.254.

Table 2. Non-dimensional numbers for atomization

	50 bar			100 bar		
	Re	We	Oh	Re	We	Oh
n-decane 25°C	8,523	15,315	0.01452	9,360	19,232	0.01482
n-decane 75°C	15,254	18,689	0.00896	19,814	32,920	0.00916
n-hexane 25°C	22,322	17,227	0.00588	28,482	29,349	0.00601
n-hexane 75°C	33,058	29,450	0.00519	39,585	44,453	0.00533

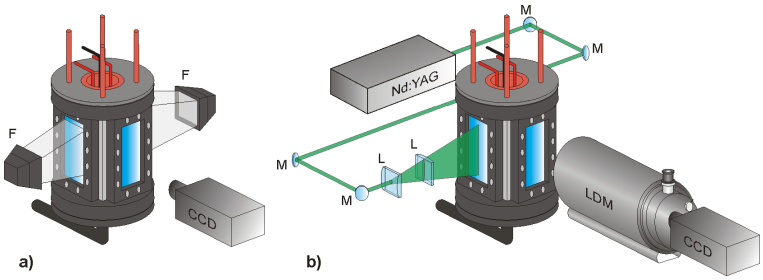

Figure 1. Measurement alignment to study the integral spray structure (a) and microscopic structure close to the nozzle with a Long Distance Microscope (LDM), illuminated with a laser light sheet (b); F=Flash-lamp, L=Lens, M=Mirror

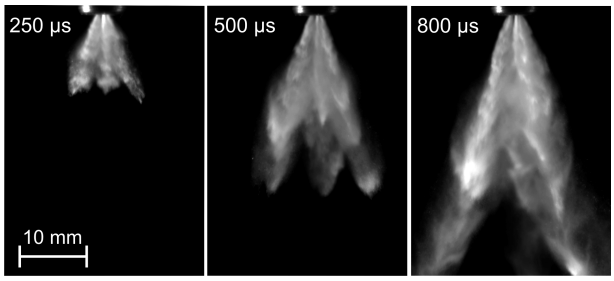

Figure 2. Integral spray illumination with flash lamps to study global spray behavior of the 3-hole nozzle

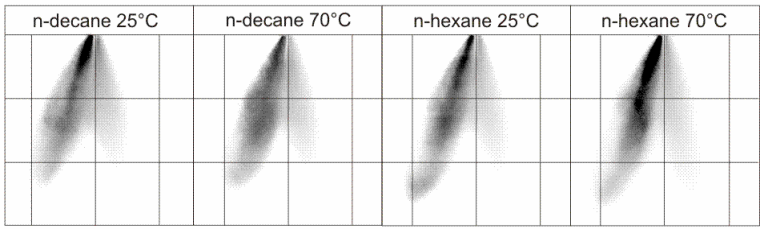

Figure 3. Macroscopic spray behavior of a single jet which is illuminated by a laser light sheet; averaged images, grid spacing is 10 mm; p_{inj} = 100 bar, p_c = 1 bar, 400 µs after visible start of injection (a. v. SOI)

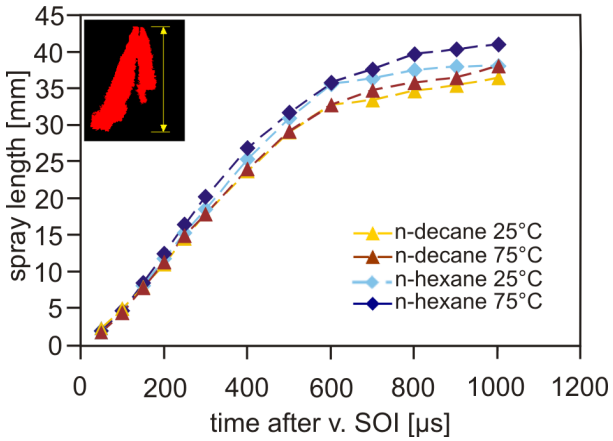

Figure 4. Vertical spray length of the laser light sheet illuminated jet, p_{inj} = 100 bar

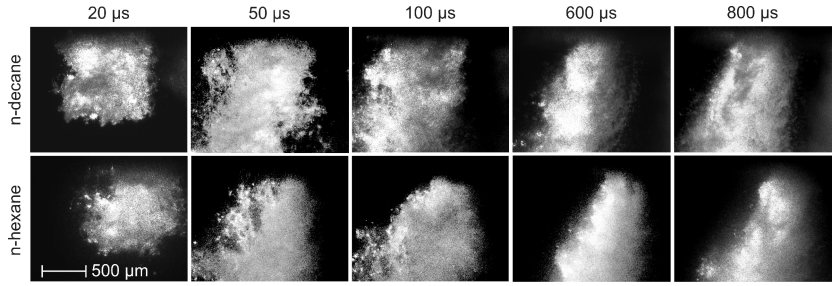

Figure 5. Microscopic spray images taken 1 mm below nozzle exit, laser light sheet illuminated jet, p_{inj} = 100 bar, ϑ_{fue} = 25°C

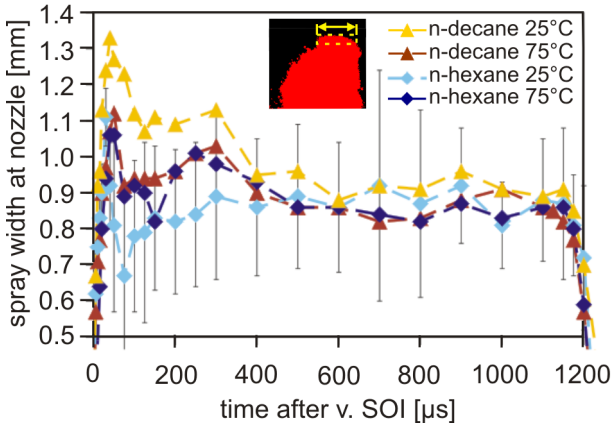

Figure 6. Averaged microscopic radial spray width at the nozzle exit, p_{inj} = 100 bar, p_c = 1 bar,

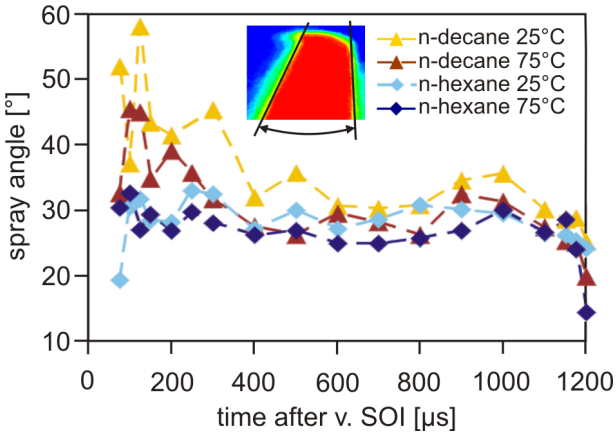

Figure 7. Microscopic spray angle at the nozzle exit (determined for the probability density function of the liquid fuel distribution); p_{inj} = 100 bar

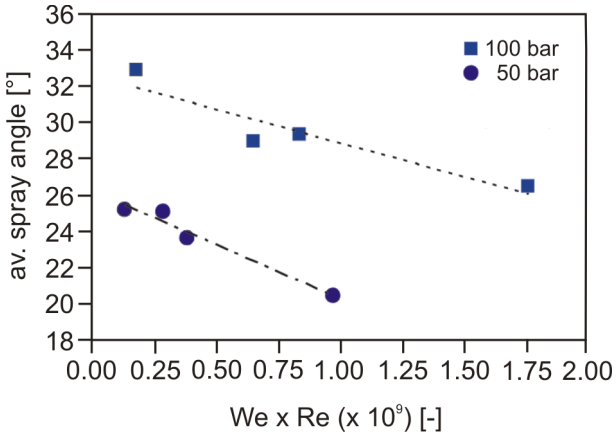

Figure 8. Averaged microscopic spray angle at the nozzle exit for the quasi-stationary phase (500-1,000 µs) depending on the injection conditions